Quantifying precipitation suppression due to air Pollution

First author: Amir Givati
The Hebrew University of Jerusalem, Jerusalem, Israel

Second author: Daniel Rosenfeld
The Hebrew University of Jerusalem, Jerusalem, Israel

Corresponding author: Daniel Rosenfeld
Contact information for the corresponding author:

Daniel Rosenfeld

Institute of Earth Sciences

The Hebrew University of Jerusalem

Jerusalem 91904, Israel

Tel: Office: +972-2-6585821, Fax: +972-2-6512372

Email: Daniel.rosenfeld@huji.ac.il

Version date: 20 January 2004

ABSTRACT:

Urban and industrial air pollution has been shown qualitatively to suppress rain and snow. Here we quantify the precipitation losses over topographical barriers downwind of major coastal urban areas in California and in the land of Israel, which amounts to 15 – 25% of the annual precipitation. The suppression occurs mainly in the relatively shallow orographic clouds within the cold air mass of cyclones. The suppression that occurs over the upslope side is coupled with similar percentage enhancement on the much drier downslope side of the hills. The evidence includes significant decreasing trends of the ratio of hill/coast precipitation during the 20th century in polluted areas in line with the increasing emissions during the same period, whereas no trends are observed in similar nearby pristine areas.

The evidence suggests that air pollution aerosols that are incorporated in orographic clouds slow down cloud-drop coalescence and riming on ice precipitation, hence delaying the conversion of cloud water into precipitation. This explains the pattern of greatest loss of precipitation at the mid-level of the upwind slopes, smaller losses at the crest, and enhancement at the downslope side of the hills.

1. Introduction

The objective of this study is the first-ever quantification of the microphysical effect of air pollution aerosols on precipitation on a regional scale (tens to several hundreds of kilometers). Previous studies have shown qualitatively that urban and industrial air pollution suppresses precipitation-forming processes in convective clouds (Rosenfeld, 1999, 2000). The pollution aerosols serve as small CCN that form large concentrations of small cloud droplets. This in turn suppresses the drop coalescence and the warm rain processes, as well as the ice precipitation (Rosenfeld, 2000, Borys et al., 2003) and so prolongs the time required to convert the cloud water that exists in small drops into large hydrometeors that can precipitate. Borys et al. (2003) show that the addition of as little as 1 $\mu g\ m^{-3}$ of anthropogenic sulfate aerosols to a clean background can reduce the orographic snowfall rate in the Colorado Rocky Mountains by up to 50%. The suppression is stronger in shallower clouds with warmer top temperatures. Satellite observations showed that pollution can completely shut off precipitation from clouds that have temperatures at their tops > -10ºC (Rosenfeld and Woodley, 2003). Therefore, it is expected to find the greatest rain suppression in regions that are dominated by relatively short living clouds with relatively warm tops downwind of major urban areas. Due to their short life, such clouds are more sensitive to slowing down of the conversion of cloud water to precipitation, whereas long living clouds would eventually convert their water into precipitation regardless of the conversion rate. The urban heat island has been documented previously as the main cause for precipitation enhancement in the warm season downwind of major urban areas (Changnon, 1979; Changnon et al., 1991; Shepherd et al., 2002). Therefore, we had to select regions where the precipitation is dominated by clouds that are not

thermally driven, preferably formed by orographic lifting over mountain ranges downwind of pollution sources during the cold season. We used annual rainfall data because almost all the precipitation in the areas of interest occurs in the winter or in winter-like storms during the spring and autumn.

2. The study areas and data collections

Ideally, the effect would be most pronounced downwind of coastal cities with hills inland that receive precipitation mainly during the winter in maritime onshore flow from shallow convective clouds. The main effect would be, therefore, the suppression of the orographic component of the precipitation, which would be manifested as a reduction in the orographic enhancement factor Ro, where Ro is defined as the ratio between the precipitation amounts at the hills and at the upwind lowland. Such conditions are quite abundant, especially on the west coast of continents in the subtropics and mid-latitudes, where the precipitation over the hills is a major source for the scarce water there. This study analyzes historical records of precipitation from California and from the land of Israel, as representative of these conditions (see maps in Fig 1).

The main analysis tool is the time series of Ro based on annual precipitation from rain gauges downwind and side wind of major urban areas. The underlying assumption is that small particulate air pollution emissions have increased with the growth of the urban areas, resulting in a decrease in Ro with time. The side wind Ro time series are not expected to show any trend with time, and so serve as controls.

3. Results and discussion

3.1. Trend analyses of rain gauges

Figs. 2-5 display the longest annual time series that could be found in California and in the land of Israel for urban down wind and side wind pairs of rain gauges. According to Fig. 2D Ro decreased by 28% in the mountains to the east of San Diego during the 20th century, most of it after 1940, when San Diego started to grow, and more recently with the explosive growth of Tijuana just across the Mexican border. No such decrease could be detected farther north in the midway between San Diego and Los Angeles, but a decrease has occurred again downwind of the Los Angeles (Fig. 6a), Fresno and San Francisco areas. Farther north, in the sparsely populated northern California, again no decreasing precipitation trends were observed (Fig. 3C), or even some statistically insignificant increases. A similar situation is evident in the land of Israel (Figs 4D, 5D). These trends occurred consistently in all the pairs of rain gauges that were tested, and summarized in the tables in the appendix. The decreasing trend of Ro does not necessarily mean absolute decrease of precipitation, since the precipitation decreases may have occurred in the context of long-term increases in the overall precipitation (See absolute trends in figures 2A, 2B, 3A, 3B, 4A, 4B, 5A, 5B).

Many more rain gauges have been available for such trend analysis for the last 60 years, making it possible to compare clusters of rain gauges in the hill and upwind plain areas. Their analysis shows a clear signal of decreasing Ro in the San Diego, Los Angeles and San Francisco areas and in and central Israel. Additional analyses other areas in California and in the land of Israel (see Appendix) show that the decreasing trends occur at the western slopes of the hills that are located downwind of pollution

sources. Again, such a trend was not found in hills downwind of pristine areas. The continuous decrease of Ro is consistent with the increasing trend of air pollution in Israel throughout the period. However, the values of standard air quality measurements in California have improved since the late 1970's (Malm et al. 2002) while Ro continues to decrease at a somewhat lesser rate, as shown in the appendix. This raises a question whether it is really the particulate air pollution that is responsible for the observed trends in Ro.

3.2. The radiosonde model

The most likely alternative explanation to the reduction in Ro is a decreasing trend in the cross-mountain component of the low tropospheric wind velocity and moisture flux during rain events. Orographic precipitation has already been related quantitatively to the low level winds and moisture both in California (Pandey et al., 1999; Neiman et al., 2002) and in the land of Israel (Alpert and Shafir, 1991; Rosenfeld and Farbstein, 1992). We applied the radiosonde regression model after Rosenfeld and Farbstein (1992) to predict the daily rain amounts in the hilly stations, where the upwind coastal precipitation and the cross-mountain 850 hPa wind velocity and the absolute humidity at that level are:

RMM = RCM (WS*W)

Where:

RMM is the predicted precipitation in the mountains [mm day^{-1}].
RCM is the gauged precipitation at the coast [mm day^{-1}].
WS is the wind speed component toward the mountain [m s^{-1}].
W is the Mixing ratio (g kg^{-1}).

Radiosonde data have been available since the early 1950's for both California and Israel. The model results show that the ratio between the actually measured rain and the predicted rain (which is unaffected by pollution) for polluted mountain areas decreased both in California and in Israel very similarly to the observed trends of Ro. The model results for clean areas show no difference between the measured rain and the predicted rain. Essentially, this reflects that the relevant meteorological conditions during rain days did not change systematically along the years, and the observed trends in Ro are likely caused by non-meteorological reasons, such as anthropogenic air pollution.

3.3. Aerosol properties

In line with these considerations, in spite of the reported decreases in the pollutant emissions in California during the last two decades, the total amount of soluble pollution ions in precipitation particles aloft have not shown any decreasing trend and even a slight increasing trend in Sequoia National Park (Table 1). Therefore, the expectation for a recent recovery of Ro with the improving standards cannot be supported by these observations of the recent trend of steady to increasing concentrations of pollution in the precipitation. The contaminants in the precipitation were monitored in the Sierra Nevada at elevated locations that eliminated the possibility of scavenging the pollutants below cloud base, because the monitoring stations were mostly above cloud base level during precipitation events. Local sources for pollutant species such as SO_2, Nox and NH_3 were found to be relatively unimportant in the Yosemite and Sequoia national parks, and were attributed to transport from the urban areas and from the oil industry in the southern San Joaquin Valley (Collett, 1989; Collett, 1989 et al;

Collett, 1990 et al, Takemoto et al, 1995; Carroll et al, 2002). Indeed, the combined concentrations of non-sea salt ions in the precipitation (Ca, Mg, K, NH_4, NO_3, SO_4), at the mountain stations of the Sierra Nevada, showing a significant decreasing trend of precipitation (Fig. 7), were twice the concentration found at the northern Sierra, where no trend in Ro is indicated (see Table 1). These ions, especially sulfates and nitrates, are major constituents of pollution-produced CCN particles.

3.4. Trend of very small CCN

A prime suspect for the lack of recovery of Ro, despite the decreasing levels of standard measures of air pollution in California, is the constancy of the very small aerosols that account for the bulk of the CCN concentrations. A major source of very small (<0.1 μm) aerosols, which are as efficient as CCN as biomass smoke particles, is diesel engines (Lammel and Novakov, 1995). A diesel car produces several orders of magnitude more such particles per mile than a gasoline car with the same fuel consumption (Pierson and Rachaczek, 1984; Williams et al, 1989; Lowenthal et al, 1994; Weingartner et al, 1997; Maricq. et al., 1999). The consumption of diesel fuel in transportation has been increasing in California at twice the pace of gasoline since 1980, and respectively the production of these small CCN aerosols, which are not reflected in any of the standard air quality measures. Furthermore, these small and numerous particles have the greatest potential for precipitation suppression. In contrast, the larger (> 1 μm) pollution particles could actually induce large drops and enhance precipitation, but these are the particles that have been most effectively eliminated from the emissions.

3.5. Classification by synoptic conditions

The next step focused on the cloud types that are most vulnerable to the suppression effects. We expect that most strongly affected would be the clouds forming in the cold sector of the cyclone, because their roots are near the surface so that they can readily ingest the air pollution, as was found by Dayan and Lamb (2003). In addition, the cloud top temperatures in the cold sector are typically much higher than for the frontal and warm sector clouds. The roots of the latter clouds are usually not connected directly to the surface, especially in the cold season, but rather feed on long-range transport of moisture. These frontal and warm-sector clouds are forced typically by synoptic lifting, so that their formation is much less dependent on orographic lifting than the clouds in the cold sector, which enjoy little synoptic forcing. Because all that we had to work with is the radiosonde data, we divided the rain days into “warm” and “cold” classes, delimited at a temperature of -3ºC at 700 hPa. This threshold was selected because it is the highest temperature that would still allow convection through that level starting from a typical winter sea surface temperature of 15ºC off the coast of southern California. According to Fig. 7, the orographic enhancement was much greater (by a factor of five at the start of the period and a factor of 3.28 at the end) for the clouds in the colder situation. Respectively, Ro for the clouds in the cold conditions showed a strong decrease (E/S = 3.28/5.00) in accordance with our conceptual expectations, although not statistically significant because of the large scatter. The scatter of the points for the warmer conditions is much smaller, in agreement with the large degree of organization of the frontal and synoptically

forced cloud systems versus the poorly organized post frontal clouds, which is responsible for the large scatter and the lack of statistical significance in the colder conditions. Similar analysis could not be done for Israel because almost all rainfall there occurs from the cold air masses. Nevertheless, this might explain the rather large effect in Israel in spite of the modest height (up to 1 km) of the hills.

3.6. Trend analyses of mountain snow pack water content

All the analyses presented up to this point suggest that anthropogenic aerosols suppress the orographic precipitation in stations located at elevations < 2 km on the upwind slopes of topographic barriers. The next natural question is what happens when the clouds are forced across very high barriers and reach very cold temperatures, where aerosols suppress precipitation to a lesser extent because ice

precipitation processes become more efficient. The answer for that was obtained from end-of-winter measurements of the water value of the snow pack near the divide of the Sierra Nevada downwind of Sacramento and Fresno. These data showed only a small (7-8%) and statistically insignificant decreasing trend of Ro. To make sure that air pollution was still delaying the formation of precipitation in these clouds, the trend of Ro farther upwind and at lower elevations was tested and found to decrease strongly (22 – 24%) and highly significantly (Fig. 8). Similar analysis in pristine areas in northern California showed near zero to slightly positive trends of Ro at all elevations (see Appendix).

3.7. Downslope compensating effects

Next, we explore the question of what happens downwind of the ridgeline to the excess cloud water that was not converted into precipitation due to the suppression of precipitation on the upslope side. Apparently the added cloud water and newly formed precipitation particles that pass over the divide cause enhancement of the precipitation on the downslope side. This occurs in all areas with available data where suppression was observed on the upslope side, both in California and the land of Israel (see example in Figs. 8,9). No trends in Ro were found at the upslope and downslope of hills downwind of pristine areas. The opposite trends on the western and eastern slopes downwind of pollution sources are of comparable magnitude in percentage, but because the absolute amount of precipitation over the western slope is about 4 times greater than over the eastern slope (in the case shown in Fig. 9), the net result is dominated by the decrease of Ro over the western (upwind) slopes.

4. Summary of the results

Figs 10, 11 and 12 summarize the results both in California and the land of Israel. Fig 10 displays on a map the trends in Ro in polluted areas downwind of Sacramento, Fresno and Los Angeles in California, and in the Samaria and Judea hills, the land of Israel. The trend of Ro is denoted as E/S in the figures, which means period-ending / period-starting Ro. In fig 11 it can be seen that no such trend accrued in pristine areas that are located north of San Francisco and in the Hebron mountains, the land of Israel. Fig 12 shows in a schematic cross section from west to east the full process as it accrues in the polluted mountain of the Sierra Nevada,

California (downwind to Fresno). It can be seen that the western slopes are the most sensitive areas to air pollution effect. The decrease in the orographic ratio between the coastal and plains area to them is around 20% (statistically significant). This trend becomes weaker as we rise up in elevation and the opposite trend occurs in the eastern slopes of the Sierra Nevada. The proportion of the post frontal precipitation from the colder air masses, which is more orographically controlled (see Fig. 7), has not decreased with time at all, especially at the coastal stations. For example, the fraction of rainfall that occurs with 700 hPa T<-3^{o}C, which is associated with the more orographic rainfall, has increased between 1952 and 2000 from 52% to 57% in San Diego while decreasing from 73% to 72% in Cuyamaca (See detail in the Appendix). This does not leave any conceivable alternative mechanism that the authors are aware of, except for the aerosol effects that can explain the observed patterns of suppression of the orographic component of the precipitation at the upslope side of the western slopes, while increasing it on the eastern slopes.

An important question is the net gain or loss of precipitation along the whole cross section. This is calculated in Table 2 for a 1-km wide strip across the average width of the Sierra Nevada stages with their respective rainfall changes as defined in Fig. 12. The reduction in the western slopes dominates the overall hydrological budget, incurring a large net loss, of about 20 million m-3 for each 1-km segment of the mountain ranges. This means an overall loss of $4x10^{9}$ m^{3} $year^{-1}$ of precipitation water just for the 200 km long section of the mountains that are located to the east of the line between Sacramento and Fresno. This calculation is highly oversimplified and provides us merely with the magnitude of the problem. More exact calculations and their hydrological meaning are in required. Further,

these precipitation losses may not even be evident to water managers because of masking by the long-term increases in the overall upwind base level of precipitation.

In this study we analyzed only two geographical areas where we had the physical basis to expect that such unfavorable redistribution of precipitation occur, and had quality precipitation data at the hilly areas available to us. Similar effects can be expected in other areas, such as the Snowy Mountains and Victorian Alps in Australia (Rosenfeld, 2000), The Atlas Mountains, Mediterranean coastal hill ranges, Chille, Puerto Rico, and many more locations.

In this study we avoided dealing with the possible confounding effects of the glaciogenic cloud seeding of the orographic clouds that have been taking place in both Israel and California. If seeding did enhance precipitation, the results in the absence of seeding may have been worse than indicated in this study. Additional research is needed to separate the seeding and pollution effects. In addition, measurements of CCN are needed to strengthen to case for pollution as causal of the apparent losses in precipitation.

5. Conclusions

In summary, strong circumstantial evidence links quantitatively anthropogenic air pollution and suppression of orographic precipitation downwind of the pollution sources by 15 to 25%, in the following ways:

- The decreasing trend is linked to the period of urbanization and industrialization upwind, whereas similar analysis of the orographic rainfall in nearby pristine areas showed no trends.

- The suppression occurs mainly in the relatively shallow clouds within the cold air masses of cyclones, which ingest the pollution from the boundary layer while ascending over the mountains.
- The suppression that occurs over the upslope side is coupled with similar percentage enhancement on the much drier downslope side of the hills, probably because more cloud water passes over the divide.

The main hydrological recharge zones of the water resources in the study areas overlap with the areas where large and statistically significant suppression of precipitation was measured, with water losses ranging between 15 and 25% of the annual precipitation. The downwind areas where compensatory enhancement occurs have much lower absolute amount of precipitation (about 25%) than the upslope side of the hills, and therefore the compensatory relative increases on the downwind side are manifested as much smaller amounts of added water compared to the losses in the upslope areas. For example, a net loss of precipitation water volume of about $4x10^9$ is estimated over the mountains to the east of the line connecting Fresno and Sacramento. These are startling results for regions that already now experience severe water shortages and have to resort to seawater desalination (in Israel) to meet their water needs. In addition to the obvious ramifications to water resources, climate impacts are also important and must be considered.

Acknowledgements

This study was funded by the Israeli Ministry of Science and by the Eshcol Foundation. The authors thank Dr. W. L. Woodley for valuable discussions and reviewing the manuscript.

List of Figures:

Figure 6 : Recent trends in the annual ratio of precipitation (Ro) between clusters of 5 to 7 gauges in the hills and the upwind urban area of (A) Los Angeles in California, and (B) the Judean hills vs. the Israel central coastal plain. The small P values show that the trends are statistically significant. Station details are in the appendix.

Figure 7: The annual ratios of precipitation (Ro) between Cuyamaca and San Diego for clouds occurring when T>-3ºC at 700 hpa (mainly frontal and warm air mass) and when T $\leq$ -3^{o}C (mainly cyclonic post frontal clouds).

Figure 8: The annual ratios of precipitation (Ro) between the western slopes of the Sierra Nevada and the upwind lowlands, represented by (A) Pacific House versus Fresno and (B) Giant Forest versus Fresno. The Ro of the water value of snow pack at highest western slopes of the Sierra Nevada is represented by Alpine cluster (Sonoma pass, Bond pass, Carson pass) versus Sacramento (A) and the cluster near the Divide above Sequoia-Kings National Park (Mono pass, Piute pass, Kaiser pass, Emerald Lake) versus Fresno (B). The relative compensation in the eastern slope is shown in B by Ro of Bishop Lake with respect to the Divide cluster. The locations of the stations in A and B are shown in the blue frames A and B of Figure 1 and in maps A and B of Figure 10, respectively.

Figure 9: The annual ratios of precipitation (Ro) of rain gauges on the western slopes (Lake Arrowhead, 1740 m, 1033 mm/year, 22C in Fig.1) and eastern slopes (Morongo, 915 m, 244 mm/year, 23C in Fig 1) of the mountains to the east of Los Angeles with respect to the rainfall in Los Angeles. Note that the decreasing trend on the western slope is coupled with an increasing trend on the eastern slope.

Figure 10: Summary of trends in precipitation ratios in cross sections downwind of urban areas. Map A shows the ratios of annual precipitation (Ro) for "polluted" rain gauges at a cross section downwind of Sacramento (6A in fig. 1) through the Pacific House (1147 m, 1308 mm/year) at the western slopes of the Sierra Nevada (7A in fig. 1), Cluster of snow pack stations (2953 m, 945 mm/year) at the divide in Alpine county (8A in fig. 1), Woodfords (1890 m, 533 mm/year) at the eastern slopes of the Sierra Nevada (9A in fig. 1). Map B shows a cross section downwind of Fresno (10B in fig. 1) through Grant Grove (2283 m, 1062 mm/year) at the western slopes of the Sierra (11B in fig. 1), cluster of snow pack stations (averaging 2953 m, 926 mm/year) in Sequoia-King N.P (12B in fig. 1), Glacier (2733 m, 406 mm/year) in the eastern slopes (13B in fig. 1), and Bishop Lake (3767, 546

mm/year) high in the eastern slopes (14B in fig. 1). Map C shows a cross section downwind of Los Angeles (19C in Fig. 1) through Lake Arrowhead (1740 m, 1033 mm/year) at the western slopes (21C in Fig. 1), Morongo (915 m, 244 mm/year) in the eastern slopes (23C in fig. 1). Map D shows a cross section downwind of Tel Aviv area (1D in Fig. 1) through a cluster of stations (660 m, 671 mm/year, 2D in Fig. 1) in the Samaria hills, and Biet Dajan (520 m, 320 mm/year, 3D in Fig. 1) in the eastern slopes. It also shows a cross section from a cluster of stations in the Israeli internal plain (180 m, 521 mm/year, 7D in Fig. 1) to a cluster of stations in the Judea hills (743 m, 650 mm/year, 6D in Fig. 1).

Fig 11: Same as fig. 10 but for a relatively pristine area. Map E shows the ratios of annual precipitation (Ro) in cross sections downwind of pristine areas in Northern California for Ukiah (208 m, 970 mm/year, 1E in fig. 1) through Bowman in the western slopes (2000 m, 1712 mm/year, 3E in fig.1), to Boca in the eastern slopes (1858 m, 572 mm/year, 4E in fig.1). Map F shows a cross section for two pairs of pristine stations to the north of Los Angeles: of Mt. Figuroa **(**1066 m, 508 mm/year, 16F in Fig. 1) versus Santa Barbara (33m, 524 mm/year, 15F in Fig. 1), and Mt. Pine (1400m, 575 mm/year, 18F in Fig. 1) versus Santa Barbara (33m, 524 mm/year, 17F in Fig. 1). Map G shows a cross section for Hebrom (1000 m, 560 mm/year, 9G in fig.1) in the Hebron hills versus Ruhama (150 m, 354 mm/year, 8G in fig.1), which is in Israel's southern plain and.

Fig 12: Topographic cross section showing the effects of urban air pollution on precipitation as the clouds move from west to east from the coast to the Sierra Nevada Mountains and to the eastern slopes. The boxes show the amount of the annual precipitation (mm/year) in each topographic location and the numbers above them show the loss or gain of precipitation (mm/year) at each site. Maritime air (zone 1) is polluted over coastal urban areas (zones 2, 3) - No decrease in precipitation occurs. The polluted air rises over mountains downwind and forms new polluted clouds (zone 4) –decreases of 15% -20% (losses of 220 mm/year) in the ratio between the western slopes to the coastal and plain areas. The clouds reach to the high mountains (zone 5). All the precipitation is snow – slight decrease of 5% to 7% (loss of 65 mm/year) in the ratio between the summits to the plain areas. The clouds move to the high eastern slopes of the range (zone 6) - increase of 14% (gain of 66 mm/year) in the ratio between the eastern slopes to the plain. According to Table 2 the net loss is dominant.

Appendix

This appendix contains additional information about the graphs that are presented in this paper. In addition, many more cases and results from California and the land of Israel are brought here in order show that the results that are presented in the paper are examples for the general situation. The appendix includes 13 tables. Each table describes different aspects, which together help to show the full picture of the time series that we present.

Each table contains the following information: Station name, Long / Lat, Years, Elevation, Average annual precipitation, Correlation, Ending / Starting ratio, P-value, Ending / Starting precipitation.

Explanation for the tables entries:

1. Stations name: The rain gauges or snow pack name.

2. Long / Lat: The geographical longitude and latitude [in decimal degrees].

3. Years: The analyzed period in starting and ending years.

4. Elevation: The elevation of the rain gauges or snow packs in meters above sea level.

5. Average yearly precip. : The average annual amount of precipitation in each station for the tested years [mm/year].

6. Correlation: The correlation coefficient between the annual rainfall of pairs of stations.

7. Ending / Starting ratio: The ratio (where the ratio is defined as the ratio between the precipitation amounts at the hills and at the upwind lowland) in the beginning of the time series comparing to the ratio in the end gives the change, as calculated using the regression line. This is the trend along the years.

8. P value: The statistical significance of the trend corresponds to the t test statistic. It means the probability of the indicated trend occurring just due to the random variability, and not due to a real trend.

9. Slope: The slope that is calculated for the trend from the regression equation.

10. Ending / Starting precipitation: Same as ending / starting ratio but for individual rain gauges time series, not for pairs of station ratios.

11. Cluster: Group of rain gauges or snow packs that represent the average annual precipitation in a selected geographical area.

Appendix Table 1: Trend analysis for station ratios – No orographic factor						
Stations name[1]	**San Bernardino**	**Los Angeles**	**Sacramento**	**San Francisco**	**Cluster of stations in Judea plains** * App. Table 2 shows the list of the stations	**Ashdod**
Long / Lat [Decimal][2]	-117.279/34.160	-118.237/34.053	-121.480/ 38.583	-122.417/ 37.783	34.834/ 31.746	34.39/ 31.500
Years[3]	1880 – 2000		1945 – 2000		1950 - 2000	
Elevation [m][4]	367	100	9	17	180	50
Average yearly precip. [mm][5]	394	343	475	538	521	520
Correlation[6]	0.82		0.88		0.88	
Ending / Starting ratio[7]	1.20 / 1.19 = 1.01		1.15 / 1.15 = 1.00		1.02 / 1.02 = 1.00	
P value[8]	0.82		0.90		0.98	
Slope[9]**:1945- 2000**	0.0005 (1880-1944)		0.0004		- 0.0001	
Ending / Starting ratio:1945-1974	1.20/1.21=0.99 (1880-1944)		1.13/ 1.15= 0.98		1.00/1.02 = 0.98 (1950-1974)	
P value:1945-1974	0.84 (1880-1944)		0.60		0.72	
Slope:1945 -1974	-8E-05 (1880-1944)		-0.002		-0.0015	
Ending/ Starting ratio: 1974-2000	1.20/1.21=0.99		1.14/1.09 =1.04		1.00/1.04 = 0.96	
P value:1974-2000	0.78		0.36		0.55	
Slope:1974 -2000	-0.006		0.013		-0.008	

Appendix Table 2: List of stations: Cluster of stations in Judea plains – No orographic factor					
Station name[1]	**Nahshon**	**Hulda**	**Zora**	***Yesodot***	***Mishmar David***
Long / Lat[2] [Decimal]	34.574/31.505	34.909/31.841	34.959/31.748	34.834/31.821	34.898/31.817
Elevation[4] [m]	200	125	350	70	155
Average yearly precip.[5] [mm]	507	536	493	547	486

Note: Radar observations showed that during post cold frontal rain events the orientation of the cloud movement was from west to east, with an average azimuth of 260 degrees (Rosenfeld, 1980). It means that the clouds move from the pollution sources in the coast to the Judea and Samaria mountains, and from the relatively clean area in the southern coast to the Hebron hills.

Rosenfeld, D., 1980: Characteristics of Rainfall Cloud Systems, Radar and Satellite Images Over. M.Sc. Thesis, Dept of Atmospheric Sciences, Hebrew University, Jerusalem.

Appendix Table 3 : Trend analysis for station ratio: Mountain / coast stations – Clean area								
Stations name[1]	**Bowman**	**Ft Bragg**	**Mt. Pine**	**Santa Barbara**	**Hebron**	**Ruhama**	**Mt. Figuroa**	**Lompoc**
Long / Lat[2] [Decimal]	-120.656/ 39.613	-123.807/ 39.613	-119.364/ 34.609	-119.700/ 34.417	35.060/ 31.320	34.422/ 31.301	-120.006/ 34.736	-120.474/ 34.663
Years[3]	1945 - 2000		1949 - 1997		1949 - 1997		1949 - 1997	
Elevation[4][m]	2000	27	1400	33	1000	150	1066	40
Average yearly precip.[5] [mm]	1712	993	575	524	570	354	508	343
Correlation[6]	0.91		0.89		0.89		0.86	
Ending/ Starting ratio[7]:1945 – 2000	1.93 / 1.80 = 1.07		1.15 / 1.05 = 1.10 (1949-1997)		1.63 / 1.61 = 1.01 (1949 -1997)		1.57/1.43 = 1.10	
P value[8] : 1945 – 2000	0.46		0.13		0.98		0.50	
Slope[9] : 1945 – 2000	0.010		0.025		0.025		0.002	
Ending/ Starting ratio:1945-1974	1.98 / 1.84 = 1.07		1.10 / 1.04 = 1.05 (1949-1974)		1.60 / 1.56 = 1.03 (1949-1974)		1.60 / 1.40 = 1.14 (1949-1974)	
P value :1945-1974	0.66		0.63		0.63		0.23	
Slope : 1945 -1974	0.021		0.015		0.015		0.01	
Ending/ Starting ratio:1974-2000	2.05/ 1.79 = 1.14		1.15/1.10 = 1.05		1.67/1.64 = 1.02		1.65 / 1.58= 1.04	
P value :1974-2000	0.44		0.37		0.37		0.78	
Slope : 1974 -2000	0.090		0.027		0.027		0.001	

Stations name[1]	Lake Spaulding	Ukiah	Mineral	Ukiah	Hemet	El Toro
Long / Lat[2] [Decimal]	-120.637/39.319	-123.200/39.150	-116.676/39.350	-123.200/39.150	-116.676/33.669	-117.700/33.600
Years[3]	1895-2000		1930-2000		1896-2000	
Elevation[4][m]	1718	208	1452	208	1452	125
Average yearly precip[5]. [mm]	1822	970	1397	970	499	362
Correlation[6]	0.87		0.94		0.84	
Ending/ Starting ratio[7] 1895-2000	1.85/1.85 = 1.00		1.50/1.50 = 1.00 (1945-1995)		1.41/1.35 = 1.04	
P value[8]	0.86		0.87		0.55	
Slope[9]	0.0001		- 0.0008		0.001	
Ending/ Starting ratio:1895 -1945	1.85/1.85 = 1.00		1.40/1.50 = 0.93 (1945-1974)		1.36/1.38 = 0.98	
P value :1895-1945	0.98		0.47		0.81	
Slope : 1895-1945	0.001		- 0.021		0.020	
Ending/ Starting ratio:1945-2000	1.90/1.85 = 1.03		1.50/ 1.37 = 1.09		1.46/ 1.37 = 1.06	
P value :1945-2000	0.47		0.75		0.34	
Slope : 1945-2000	0.004		0.010		0.007	

Appendix Table 4: Trend analysis for station ratio: Mountain / coast stations – "Polluted" area						
Stations name[1]	**Pacific House**	**Sacramento**	**Giant Forest**	**Fresno**	**Cluster[11] of Mt. stations in Los Angeles area** * App. Table 5 shows the list of the stations	**Cluster[11] of Plains stations in Los Angeles** * App. Table 5 shows the list of the stations
Long / Lat[2] [Decimal]	-120.656/ 39.613	-121.480/ 38.583	-118.770/ 36.568	-119.717/ 36.770	-117.437/ 34.215	-118.055/ 34.013
Years[3]	1945 - 2000		1945 - 1996		1945 - 2000	
Elevation[4] [m]	1147	9	2137	137	1686	107
Average yearly precip.[5] [mm]	1308	475	1114	280	890	419
Correlation[6]	0.93		0.86		0.91	
Ending/ Starting ratio[7] : 1945-2000	2.50 / 3.23 =0.78		3.50 / 4.50 =0.76		1.80 / 2.14 = 0.84	
P value[8] : 1945-2000	0.009		0.012		**0.03**	
Slope[9] : 1945-2000	- 0.012		-0.021		-0.006	
Ending/ Starting ratio: 1945-1974	2.75 / 3.20 = 0.85		3.79/ 4.73 = 0.80		2.15 / 2.74 = 0.78	
P value :1945-1974	0.11		0.07		0.06	
Slope : 1945-1974	- 0.030		-0.06		-0.023	
Ending/ Starting ratio: 1975-2000	2.75/2.79= 0.98		3.35 / 4.14 = 0.81		1.91 / 2.23 = 0.85	
P value :1975-2000	0.84		**0.002**		0.64	
Slope : 1975-2000	-0.008		-0.108		-0.016	

Stations name[1]	**Cuyamaca**	**San Diego**	**Cluster**[11] **Judea hills** *App. Table 6 shows list of stations	**Cluster**[11] **Judea plains** *App. Table 6 shows list of stations	**Cluster**[11] **Samaria hills** *App. Table 6 shows list of stations	**Cluster**[11] **Central coast** *App. Table 6 shows list of stations
Long / Lat[2] **[Decimal]**	-116.583/ 32.983	-117.133/ 32.733	35.128/31.825	34.834/ 31.746	35.208/ 32.171	34.826/ 31.982
Years[3]	1880 - 2000		1950-1996		1952-1996	
Elevation[4]**[m]**	1550	123	743	180	660	39
Average yearly Precip[5]**. [mm]**	875	290	650	521	671	551
Correlation[6]	0.83		0.96		0.91	
Ending/ Starting ratio[7]**: 1880 - 2000**	3.27 / 4.53 =0.72 (1880 – 2000)		1.17/1.38 = 0.85		1.10/1.20 = 0.90	
P value[8]**: 1880-2000**	**0.003** (1880 – 2000)		**0.0006**		**0.04**	
Slope[9] **: 1888-2000**	-0.009 (1880 – 2000)		-0.010		-0.005	
Ending/ Starting ratio: 1945-1974	3.50 / 4.00= 0.87		1.21 / 1.36 = 0.89 (1950-1974)		1.14 / 1.20= 0.95 (1952-1972)	
P value :1945-1974	0.10		**0.03**		0.26	
Slope : 1945-1974	-0.0186		0.0053		0.0053	
Ending/ Starting ratio: 1975-2000	3.24 / 3.62= 0.89		1.15 / 1.28 = 0.89 (1975-1996)		1.07 / 1.20 = 0.89	
P value :1975-2000	0.07		**0.01**		0.17	
Slope : 1975-2000	-0.040		-0.020		-0.006	

Stations name[1]	**Mt Hamilton**	**San Francisco**	**Grant Grove**	**Fresno**
Long / Lat[2] **[Decimal]**	-121.650 / 37.333	-122.417 / 37.783	-118.770/ 36.568	-119.717/ 36.770
Years[3]	1882-2000		1945 - 1996	
Elevation[4]**[m]**	1402	175	2193	137
Average yearly Precip[5]**. [mm]**	670	538	1061	280
Correlation[6]	0.75		0.86	
Ending/ Starting ratio[7]**: 1880 - 2000**	1.07/1.54 =0.70		3.49 / 4.60 =0.76	
P value[8]**: 1880-2000**	**0.0002**		**0.0001**	
Slope[9] **: 1888-2000**	- 0.005			
Ending/ Starting ratio: 1945-1974	1.00/1.59=0.63		4.00/ 4.60 = 0.86	
P value :1945-1974	**0.00006**		0.07	
Slope : 1945-1974	- 0.015		-0.015	
Ending/ Starting ratio: 1975-2000	1.12/1.14 = 0.98		3.00 / 4.14 = 0.72	
P value :1975-2000	0.80		**0.002**	
Slope : 1975-2000	- 0.005		-0.043	

Appendix Table 5: Trends analysis for station ratios: "Polluted" area , CA

Each mountain station is against the Cluster[11] of Plain stations in Los Angeles

Trends of Mountain stations					
Station name[1]	**Lake Arrowhead**	**Sierra PH**	**Big Bear Dam**	**Crystal 28**	**Cender Sp**
Long / Lat[2] [Decimal]	-117.187/ 34.25	-117.246/ 34.200	-116.975/ 34.242	-117.837/ 34.327	-117.876/ 34.356
Elevation[3][m]	1740	1000	2272	1923	2260
Average yearly precip[5]. [mm]	1033	781	876	882	722
Ending/Starting ratio[7]:1945- 2000	2.51 / 3.17 = 0.80	2.04 / 2.31 = 0.88	1.76 / 2.36 =0.75	2.36 /2.68 = 0.88	2.00 / 2.60 = 0.77
P value[8] : 1945-2000	**0.008**	0.17	**0.001**	**0.04**	**0.05**
Slope[9] :1945 -2000	- 0.027	- 0.012	- 0.027	- 0.028	- 0.012
Ending/Starting ratio:1945-1974	2.42/3.50=0.73	1.82/2.26=0.80	2.40/3.07 =0.78	2.00/2.57=0.78	1.81/2.41=0.76
P value : 1945-1974	**0.02**	0.11	**0.03**	0.16	**0.01**
Slope : 1945 -1974	- 0.083	- 0.038	- 0.083	- 0.036	- 0.021
Ending/ Starting ratio: 1974-2000	1.50/1.59 = 0.94	2.10/2.19=0.96	1.80/2.02 = 0.89	2.20/2.46=0.89	1.86/2.00=0.93
P value :1974 -2000	0.67	0.79	0.50	0.65	0.62
Slope : 1974 -2000	- 0.022	- 0.007	- 0.022	- 0.016	- 0.013

List of the Cluster of Coastal and Plain Stations					
Station name	**Los Angeles 355**	**Los Angeles CC**	**Los Angeles AP**	**Pomona**	**Beverly Hills 22**
Long / Lat [Decimal]	-118.095/ 34.087	-118.233/ 34.050	-118.387/ 33.942	-117.817/ 34.067	-118.399/ 34.074
Elevation[m]	103	93	35	25	85
Average yearly precip. [mm]	393	373	325	416	426

Station name	**Long Beach 224**	**San Bernardino**
Long / Lat [Decimal]	-118.191/ 33.768	-117.268/ 34.104
Elevation[m]	60	347
Average yearly precip. [mm]	290	421

Appendix Table 6 : Trend Analysis for "Polluted" stations in the land of Israel

Each mountain station is against the Cluster of Judea Plain stations

Judea hills/ Judea plain

Trend analysis of the individual stations of the Judea Hills cluster[11]

Station name[1]	**Qiryat Anavim**		**Shoresh**		**Zova**		**Biet Meir**	
Long / Lat[2] [Decimal]	35.121	31.813	35.066	31.800	35.178	31.796	35.046	31.79
Elevation[3][m]	780		680		730		530	
Average yearly precip[5]. [mm]	685		605		640		625	
Ending/Starting ratio[7]:1950-1996	1.29 / 1.46 = 0.88		1.20 / 1.32 = 0.91 * 1956-1996		1.16 / 1.36 = 0.85		1.14 / 1.29 = 0.88	
P value[8] :1950-1996	**0.01**		0.24		**0.02**		**0.003**	
Slope[9] :1950-1996	-0.0036		-0.002		-0.0042		-0.003	
Ending/Starting ratio:1950-1974	1.31 / 1.48 = 0.89		1.18 / 1.32 = 0.89		1.22 / 1.34 = 0.91		1.22 / 1.28 = 0.95	
P value :1950-1974	0.11		**0.009**		0.19		0.49	
Slope :1950-1974	-0.0076		-0.11		-0.004		-0.002	
Ending/Starting ratio:1975-1996	1.22 / 1.49 = 0.82		1.16 / 1.40 = 0.83		1.07 / 1.37 = 0.78		1.11 / 1.25=0.88	
P value :1974-1997	**0.006**		0.09		**0.03**		**0.002**	
Slope :1974-1997	-0.011		-0.011		0.015		-0.005	

Station name	***Ramalla***		***Bitonia***	
***Long / Lat* [Decimal]**	*35.197*	*31.899*	*35.163*	*31.855*
Elevation[m]	*870*		*800*	
Average yearly precip. [mm]	*707*		*653*	
Ending/Starting ratio:1952-1996	*1.09 / 1.41 = 0.77*		*1.17 / 1.32 = 0.88*	
P value :1952-1996	***0.01***		*0.08*	
Slope :1952-1996	*- 0.009*		*- 0.0028*	
Ending/Starting ratio:1952-1974	*1.20 / 1.46 = 0.82*		*1.29 / 1.26 = 1.02*	
P value :1950-1974	*0.17*		*0.47*	
Slope :1952-1974	*- 0.013*		*0.0027*	
Ending/Starting ratio:1950-1996	*1.05 / 1.31 = 0.80*		*1.10 / 1.30 =0.85*	
P value :1975-1996	*0.06*		***0.04***	
Slope :1975-1996	*- 0.011*		*- 0.009*	

List* of *Judea Plain stations

Station name[1]	**Nahshon**		**Hulda**		**Zora**		***Yesodot***		***Mishmar David***	
***Long / Lat[2]* [Decimal]**	34.574	31.505	34.909	31.841	34.959	31.748	34.834	31.821	34.898	31.817
Elevation[3][m]	200		125		350		70		155	
Average yearly precip.[5] [mm]	507		536		493		547		486	

Samaria hills / Central coast

Trend analysis of mountain stations

Station name[1]	Nablus		Sinjil		Salfit	
Long / Lat[2] [Decimal]	35.268	32.225	35.173	32.161	35.184	32.086
Elevation[3] [m]	680		775		520	
Average yearly precip.[5] [mm]	651		657		707	
Ending/Starting ratio[7]:1952-1996	1.05 / 1.20 = 0.88		1.08 / 1.20 = 0.88		1.12 / 1.20 = 0.93	
P value[8] :1952-1996	**0.04**		0.17		0.49	
Slope[9] :1952-1996	-0.0038		-0.0028		0.0038	
Ending/Starting ratio:1952-1996	1.09 / 1.27 = 0.86		1.10 / 1.30 = 0.85		1.20 / 1.18 = 1.02	
P value :1952-1996	0.14		0.16		0.52	
Slope :1952-1996	-0.0098		-0.014		0.0047	
Ending/Starting ratio:1952-1996	1.03 / 1.17 = 0.88		1.06 / 1.19 = 0.89		1.11 / 1.34 = 0.83	
P value :1952-1996	0.23		0.29		0.07	
Slope :1952-1996	-0.005		-0.008		-0.011	

List of Central Coast stations

Station name[1]	Tel Aviv		Bet Dagan		Lod		Rishon-Leziyyon		Zrifin	
Long / Lat[2] [Decimal]	34.761	32.059	34.830	31.996	34.897	31.954	34.810	31.958	34.833	31.946
Elevation[3] [m]	25		30		50		50		60	
Average yearly precip.[5] [mm]	551		555		570		522		560	

Appendix Table 7: Trend analysis for station ratios: Snow pack water content vs. Coastal stations – "Clean" area				
Stations name[1]	**Mt Lassen**	**Fort Bragg**	**Mt Shasta**	**Ukiah**
Long / Lat[2] [Decimal]	-121.303/40.281	-123.807 /39.623	-122.383 /41.717	-123.200/39.150
Years[3]	1945 - 2000		1930 - 2000	
Elevation[4][m]	2750	27	2633	200
Average yearly Precip[5]. [mm]	2032	991	1355	970
Correlation[6]	0.85		0.90	
Ending / Starting ratio[7]:1945-2000	2.20 / 2.04 =1.08		1.36 / 1.28 =1.09	
P value[8] :1945-2000	0.41		0.18	
Slope[9] :1945-2000	0.006		0.006	
Ending/Starting ratio:1945-1974	2.15 / 2.00 =1.07		1.35 / 1.29 = 1.11	
P value :1945-1974	0.42		0.26	
Slope :1945 -1974	0.011		0.010	
Ending/ Starting ratio:1974-2000	2.21 / 2.00 = 1.10		1.50 / 1.29 = 1.16	
P value : 1974 -2000	0.56		0.19	
Slope :1974 -2000	0.018		0.022	

Appendix Table 8 : Trend analysis for station ratios: Cluster[11] of snow pack water content vs. Coast stations ,CA – "polluted" areas				
Stations name[1]	**Cluster[11] of Mountain Stations In Alpine county ,CA** App. Table 9 shows the list of the stations	**Sacramento**	**Cluster[11] of Mountain Stations In Sequoia-kings N.P, CA** App. Table 9 shows the list of the stations	**Fresno**
Long / Lat[2] [Decimal]	-119.442/ 38.880	-121.480/ 38.583	-118.735/ 37.173	-119.719/36.770
Years[3]	1948 - 2000		1951 - 2000	
Elevation[4][m]	2953	8	3537	137
Average yearly precip[5]. [mm]	945	475	900	280
Correlation[6]	0.85		0.85	
Ending/ Starting ratio[7]: 1948:2000	2.00 / 2.14 = 0.93		3.17/ 3.42 = 0.92	
P alue[8]:1948:2000	0.46		0.10	
Slope[9] :1948:2000	- 0.017		- 0.015	
Ending/ Starting ratio:1948-1974	1.83 / 2.09 = 0.88		3.20/ 3.34 = 0.95	
P value :1948-1974	0.38		0.80	
Slope : 1948-1974	0.022		- 0.010	
Ending/ Starting ratio: 1975-2000	1.80 / 1.82 = 0.98		2.93/ 3.25 = 0.92	
P value: 1975-2000	0.97		0.42	
Slope: 1975-2000	- 0.001		- 0.033	

Appendix Table 9: Trend analysis of snow pack water content stations, CA – "polluted" area

Stations In Alpine county vs. Sacramento						
Station name[1]	**Sonoma pass**		**Bond pass**		**Carson pass**	
Long / Lat[2] [Decimal]	-119.59	38.417	-119.373	38.327	-119.363	38.188
Elevation[3][m]	2833		3100		2933	
Average yearly precip.[5] [mm]	889		1085		630	
Ending/Starting ratio[7]:1945-2000	1.25 / 1.39 = 0.90		2.33 / 2.33 = 1.00		1.80 / 2.05 = 0.89	
P value[8] :1948-2000	0.30		0.76		0.25	
Slope[9] :1948 -2000	- 0.008		- 0.004		- 0.013	
Ending/Starting ratio:1945-1974	1.45 / 1.45 = 1.00		2.67 / 2.25 = 1.18		2.04 / 2.00 = 1.02	
P value :1948-1974	0.47		0.23		0.85	
Slope :1948 -1974	0.017		0.035		0.005	
Ending/ Starting ratio:1974-2000	1.20 / 1.41 = 0.85		1.36 / 1.11 = 1.11		2.00 / 2.02 = 0.99	
P value :1974 -2000	0.35		0.53		0.78	
Slope :1974 -2000	- 0.024		0.030		- 0.001	

Stations. In Sequoia-kings N.P vs. Fresno								
Station name[1]	**Mono pass**		**Piute pass**		**Kaiser pass**		**Emerald lake**	
Long / Lat[2] [Decimal]	-118.463	37.263	-118.412	37.144	-119.609	37.176	-118.457	37.110
Elevation[3][m]	3817		3767		3033		3533	
Average yearly precip[5]. [mm]	780		910		985		885	
Ending/Starting ratio[7]:1945-2000	3.30 / 3.22 = 1.03		3.25 / 3.39 = 0.96		3.41 / 3.66 = 0.93		2.70 / 2.95 = 0.93	
P value[8] :1945-2000	0.91		0.75		0.77		**0.03**	
Slope[9] :1945 -2000	0.006		- 0.006		- 0.016		- 0.126	
Ending/Starting ratio:1945-1974	3.28 / 2.79 = 1.17		3.24 / 3.37 = 0.96		3.67 / 3.60 = 1.02		3.10 / 2.75 = 1.12	
P value :1945-1974	0.79		0.86		0.94		0.44	
Slope :1945 -1974	0.042		- 0.008		0.005		0.027	
Ending/ Starting ratio:1974-2000	2.88 / 3.08 = 0.94		3.10 / 3.56 = 0.87		3.30 / 3.60 = 0.91		2.70 / 2.70 = 1.00	
P value :1974 -2000	0.67		0.56		0.73		0.94	
Slope :1974 -2000	- 0.050		- 0.451		- 0.037		0.012	

Appendix Table 10: Trend analysis for station ratios: mountain / coast stations – eastern slopes - "clean" area		
Stations name[1]	**Boca**	**Bowman**
Long / Lat[2] [Decimal]	-120.080/39.388	-120.656/38.583
Years[3]	1945 – 2000	
Elevation[4][m]	1858	2000
Average yearly precip[5]. [mm]	572	1711
Correlation[6]	0.88	
Ending/ Starting ratio[7]:1945:2000	3.02/3.00 = 1.002	
P value[8] :1945-2000	0.92	
Slope[9] : 1945:2000	0.010	
Ending/ Starting ratio:1945-1974	0.75	
P value :1945-1974	3.00/3.00 = 1.00	
Slope : 1945-1974	0.003	
Ending/ Starting ratio: 1975-2000	3.00 / 3.00 = 1.00	
P value: 1975-2000	0.68	
Slope: 1975-2000	0.017	

Appendix Table 11: Trend analysis for stations ratio: East Slope / West Slope stations in "polluted" area

Stations name[1]	**Woodfords**	**Pacific House**	**Glacier**	**Grant Grove**	**Morongo**	**Los Angeles Airport**	**Biet Dajan**	**Samaria Hills Cluster** App. Table 6 shows the list of the stations	**Bishop Lake**	**Fresno**	**Bishop Lake**	**Cluster of mountain stations downwind of Fresno area** (from App. Table 8)
Long / Lat[2] **[Decimal]**	-119.820/ 38.776	-120.500/ 38.750	-118.433/ 37.126	-118.961/ 36.741	-117.173/ 33.921	118.387/ 33.942	35.364/ 32.201	35.268/ 32.224	37.123/ 118.545	18.961/ 36.741	-118.326/ 37.740	-119.442/ 37.488
Years[3]	1945-2000		1945-2000		1948 -1996		1960-1996		1951-2000		1951-2000	
Elevation[4]**[m]**	1890	1147	2733	2283	915	37	520	660	3767	2283	3767	3537
Average yearly precip.[5] **[mm]**	533	1321	406	1067	244	330	434	671	545	1067	550	900
Correlation[6]	0.86		0.86		0.70		0.88		0.84		0.89	
Ending/ Starting Ratio[7]**: 1945-2000**	0.44/0.38 = 1.16		0.48/0.38 = 1.25		0.89/0.67 = 1.33		0.67/0.56 = 1.19		2.13/1.80 = 1.18		0.82 / 0.63 = 1.28	
P value[8]**: 1945-2000**	0.09		**0.03**		0.11		0.09		0.28		**0.03**	
Slope[9] **: 1945-2000**	0.003		0.007		0.006		0.0026		0.018		0.005	
Ending/ Starting ratio:1945-1974	0.44 / 0.40 = 1.10 (1974-1990)		0.45 / 0.33=1.33		0.80 / 0.67=1.19 (49-73)		missing data		1.90 / 1.84 = 1.03		0.60 / 0.69 = 0.88	
P value : 1945-1974	**0.04**		**0.01**		0.38		missing data		0.82		0.41	
Slope : 1945-1974	0.005		0.014		0.003		missing data		0.010		- 0.008	
Ending/ starting ratio: 1975-2000	0.40 / 0.43 = 0.94		0.42 / 0.45=0.93		0.89 / 0.95 = 0.94 (74-95)		0.66/ 0.60 = 1.08 (1968 – 1994)		2.14 / 2.00 = 1.07		0.86 / 0.77 = 1.12	
P value: 1975-2000	0.15		0.46		0.42		0.44		0.26		0.28	
Slope: 1975-2000	-0.010		-0.004		- 0.0007		0.005		0.025		0.010	

Appendix Table 12 : Trend analysis for individual rain stations

Station name[1]	Cuyamaca		San Diego		Lake Spaulding		Ukiah		San Francisco		Mt. Hamilton	
Long / Lat[2] [Decimal]	-116.583	32.983	-117.180	32.730	-120.367	39.319	-123.200	39.150	-122.420	37.780	-121.650	37.330
Elevation[3][m]	1550		123		1717		2833		175		1407	
Average yearly precip.[5] [mm]	875		290		1692		208		538		595	
Ending/Starting Precipitation[10] : 1888-2000	980/ 992 = 0.90 (1888-2000)		256 / 254 = 1.01 (1888-2000)		1765 / 1584 =1.11 (1895-1945)		980 / 901 = 1.09 (1895-1945)		521 / 500 = 1.04		540 / 741 = 0.72	
P value[8] :1888-2000	0.14		0.50		0.14		0.20		0.73		**0.0001**	
Slope[9] :1888 -2000	- 0.143		0.190		0.479		0.983		0.016		- 0.224	
Ending/Starting Precipitation : 1888-1945	980 / 970 = 1.01		271 / 281 = 0.96		1535 / 1717 = 0.90		820 / 967 = 0.85		507 / 532 = 0.95		629 / 772 = 0.82	
P value :1888-1945	0.64		0.63		0.21		0.27		0.65		**0.02**	
Slope :1888 -1945	0.005		0.015		- 0.529		- 0.277		- 0.050		- 0.315	
Ending/Starting Precipitation : 1945-2000	931 / 808 = 1.15		290 / 220 = 1.32		1981 / 1686 = 1.17		1029 / 906 = 1.13		587 / 447 = 1.31		609 / 540 = 1.12	
P value :1945-2000	0.39		**0.03**		0.14		0.23		0.57		0.12	
Slope :1945 -2000	0.100		0.126		0.720		0.310		0.247		0.103	

Station name[1]	Ben Shemen		Kiryat Anavim		Fresno		Giant Forest		Bishop Lake		Cluster of mountain stations downwind of the Fresno area	
Long / Lat[2] [Decimal]	34.834	31.921	35.121	31.800	-119.717	36.770	-118.770	36.770	-118.545	37.123	-119.442	37.488
Elevation[3][m]	100		780		137		2137		3767		3537	
Average yearly precip.[5] [mm]	586		685		280		1114		546		900	
Ending/Starting Precipitation[5] : 1945-2000	600 / 500 = 1.20 (1925- 2000)		735 / 637 = 1.13 (1925- 2000)		308 / 244 = 1.26		1057 / 980 = 1.08		595 / 490 = 1.21		762 / 718 = 1.06	
P value[8] :1945-2000	0.11		0.13		0.10		0.80		0.15		0.62	
Slope[9] :1945 -2000	1.570		1.600		0.055		0.080		0.300		0.133	

Station name[1]	Sacramento		Pacific House		Cluster of Mountain stations in Alpine county		Big Bear Lake		Morongo	
Long / Lat [2][Decimal]	-121.480	38.583	-120.656	39.613	-118.735	37.173	-117.173	34.242	-116.975	33.921
Elevation[3][m]	9		1147		3537		2272		915	
Average yearly precip.[5] [mm]	475		1308		890		890		244	
Ending/Starting Precipitation[10] : 1945 - 2000	432 / 533 = 1.23		1361 / 1270 = 1.07		1016 / 940 = 1.08		838 / 925 = 0.91		184 / 307 = 1.67 (1949-1996)	
P value[8]: 1945-2000	0.11		0.75		0.39		0.56		0.13	
Slope[9]: 1945 -2000	0.230		0.113		0.240		- 0.189		0.239	

Station name[1]	Hebron		Ruhama		Cluster Judea hills		Cluster Judea plain		Cluster of Mt. stations in Los Angeles area		Cluster of Plain stations in Los Angeles	
Long / Lat[2] [Decimal]	35.060	31.320	34.422	31.301	35.128	31.825	34.834	31.746	-117.437	34.215	-118.055	34.010
Elevation[3][m]	1000		150		743		180		1686		107	
Average yearly precip.[5][mm]	560		354		650		521		890		381	
Ending / Starting Precipitation[10] : 1945-2000	600 / 513 = 1.16 (1934 – 1996)		370 / 318 = 1.16 (1934 – 1996)		657 / 600 = 1.09 (1950 – 1996)		590 / 487 = 1.20 (1950 – 1996)		787 / 735 = 1.07		419 / 333 = 1.24	
P value[8] :1945-2000	0.36		0.28		0.46		0.07		0.19		0.06	
Slope[9] :1945 -2000	2.194		0.890		1.702		2.558		0.176		1.638	

Appendix Table 13 : Trend analysis for individual rain stations during "cold" (T at 700 hpa ≤ -3°C) and "warm" (T>-3°C) air mass								
Radiosonde site	**San Diego**				**Los Angeles**			
Station name[1]	**San Diego**		**Cuyamaca**		**Los Angeles**		**Lake Arrowhead**	
Long / Lat[2] [Decimal]	-117.133	32.733	-116.583	32.983	-118.095	34.050	-117.187	34.250
Elevation[3][m]	123		1550		35		1740	
Average yearly precip. [5][mm]	290		875		373		1033	
Ending/Starting Precipitation[10] – warm sector (mm/day) : 1952-2000	16.0 / 12.7 = 1.26		25.0 / 20.2 = 1.24		23.0 / 23.2 = 0.99		19.3 / 17.8 = 1.08	
P value[8] :1952-2000	**0.02**		0.08		0.89		0.67	
Slope[9] :1952-2000	0.153		0.101		- 0.042		0.060	
Ending/Starting Precipitation[10] – cold sector (mm/day) : 1952-2000	20.8 / 13.5 = 1.54		65.5 / 55.0 = 1.18		29.1 / 20.2 = 1.43		36.8 / 30.0 = 1.20	
P value :1952-2000	**0.02**		0.46		**0.01**		0.17	
Slope :1952-2000	0.159		0.102		0.147		0.020	

References

Alpert, P. and H. Shafir, 1991: On the role of the wind vector interaction with high-resolution topography in orographic rainfall modeling. *Quart. J.R. Meteor. Soc*., **117**, 421-426.

Borys, R.D., D. H. Lowenthal, S. A. Cohn, and W. O. J. Brown, 2003: Mountain and radar measurements of anthropogenic aerosol effects on snow growth and snowfall rate. *Geophys. Res. Lett.*, **30**(10), 1538, doi: 10.1029 /2002GL016855.

Carroll, J.J., and A.J. Dixon, 2002: Regional scale transport over complex terrain, a case study: Tracing the Sacramento plume in the Sierra Nevada of California. *Atmos. Environ*., **36**, 3745-3758.

Changnon, R.T., 1979: Rainfall changes in summer caused by St. Louis. *Science,***205**, 402– 404.

Changnon, R. T., Shealy, R.W. Scott, 1991: Precipitation changes in fall, winter, and spring caused by St. Louis. *J. Appl. Meteor*., **30**, 126-134.

Collett, Jr., J.L., 1989: Characterization of cloud water and precipitation chemistry and deposition at elevated sites in central and southern California, PhD Thesis, California institute of technology, Pasadena, California.

Collett, Jr., J.L., Daube, Jr., B., Munger, J. W. and Hoffmann, M. R., 1989: Cloudwater chemistry in Sequoia National Park. *Atmos. Environ*. **23**, 999 -1007.

Collett, J.r., J.L., Daube, Jr., B. C. and M. R., Hoffmann, 1990: The chemical composition of intercepted cloudwater in the Sierra Nevada. *Atmos. Environ*. **24A**, 959-972.

Dayan, U., and D. Lamb, 2003: Meteorological indicators of summer precipitation chemistry in central Pennsylvania, *Atmos. Environ.,* **37**, 1045-1055.

Lammel, G., and T. Novakov, 1995: Water nucleation properties of carbon black and diesel soot particles. *Atmos. Environ.*, **29**, 813 - 823.

Lowenthal, D.H , zielnska B, Chow JC, Watson JG, Gautam M, Ferguson DH, Neuroth GR, Stevens KD , 1994 : Characterization of heavy-duty diesel vehicle emissions. *Atmos. Environ.*, **28** , 731-743.

Malm, W.C, Schichtel B. A, Ames R. B, 2002: A 10-year spatial and temporal trend of sulfate across the United States, *J. Geophys. Res.,* **107**, 10.1029/2002JD002107.

National Atmospheric Deposition Program. 2003.
http://nadp.sws.uiuc.edu/sites/sitemap.asp?state=CA

Neiman, J.N., Ralph P.J., White A.B., Kingsmill D.E., Persson P.O.G., 2002: The statistical relationship between upslope flow and rainfall in California's coastal mountains: observations during CALJET. *Mon. Wea. Rev*. **130**, 1468-1492.

Maricq, M.M., Chase, R. E., Podsiadlik, D.H., andVogt, R., 1999 : "Vehicle Exhaust Particle Size Distributions: A Comparison of Tailpipe and Dilution Tunnel Measurements," SAE Paper No. **1999- 01-1461**, *Society of Automotive Engineers*, Warrendale, PA.

Pandey, G.R., Cayan D.R and Georgaakakos K.P., 1999: Precipitation structure in the Sierra Nevada of California during winter. *J. Geophys. Res*. **104**, 12019-12030.

Pierson, W.R., and W.W. Brachaczek, 1983 : Particulate Matter Associated with Vehicles on the Road II. *Aerosol Sci.Technol*. **2**, 1- 40.

Rosenfeld, D., 1999: TRMM observed first direct evidence of smoke from forest fires inhibiting rainfall, *Geophys. Res. Lett* , **26**, 3105-3108 .

Rosenfeld, D., 2000: Suppression of rain and snow by urban air pollution. *Science*, **287**, 1793-1796.

Rosenfeld, D., and H. Farbstein, 1992: Possible influence of desert dust on seedability of clouds in . *J. Appl. Meteor*, **31**, 722-731.

Rosenfeld, D., and W. L. Woodley, 2002: Closing the 50-year circle: From cloud seeding to space and back to climate change through precipitation physics. Chapter 6 of *"Cloud Systems, Hurricanes, and the Tropical Rainfall Measuring Mission (TRMM)"* edited by Drs. Wei-Kuo Tao and Robert Adler, Meteorological Monographs, Amer. Meteor. Soc., p.59-80.

Shepherd, J. M., H. Pierce, A. J. Negri, 2002: Rainfall modification by major urban areas: observations from spaceborne rain radar on the TRMM satellite. *J. Appl. Metor*. **41**, 689-701.

Takemoto, B.K., Croes B.E., Brown S.M, Motallebi N., Westerdahl F.D., Margolis H.G., Cahill B.T., Mueller M.D., Holmes J.R., 1995: Acidic deposition in California: Findings from a program of monitoring and effects research. Water, Air & Soil Pollution, 85 , 261-272.

Weingartner, E, Burtscher H, Baltensperger U , 1997 : Hygroscopic properties of carbon and diesel soot particles. Atmos. Environ. , 31 , 2311-2327.

Williams, D.J., Milne J.W, Quigley S.M, Roberts D.B ,1989 : Particulate-emissions from in–use motor vehicles. Atmos. Environ., 23 , 2647-2661.

List of Figures:

Set of Figures

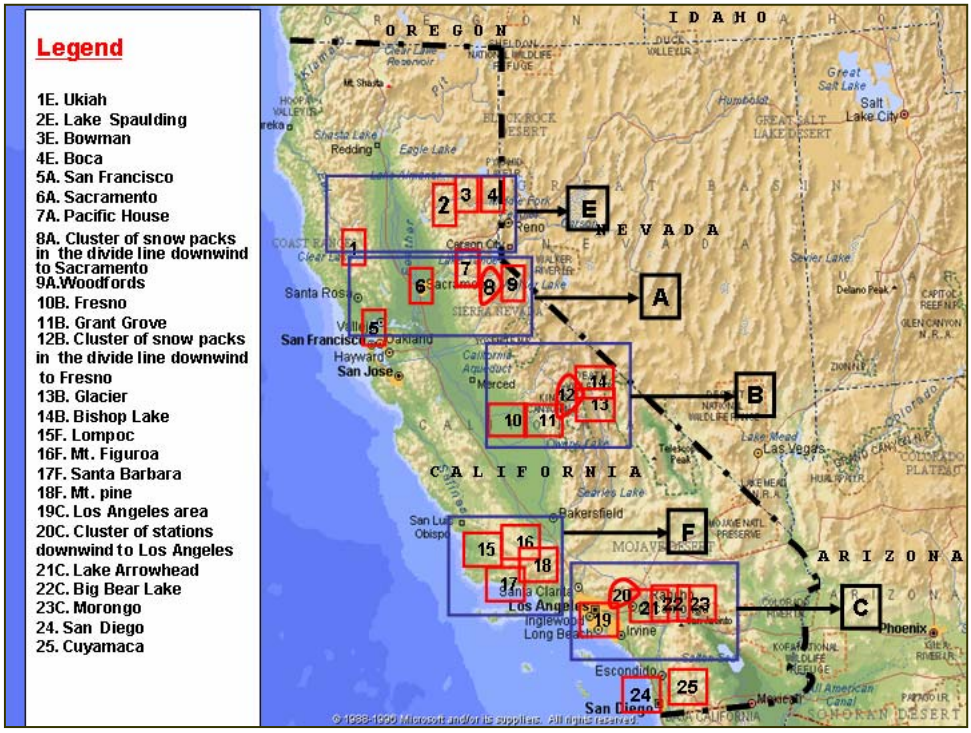

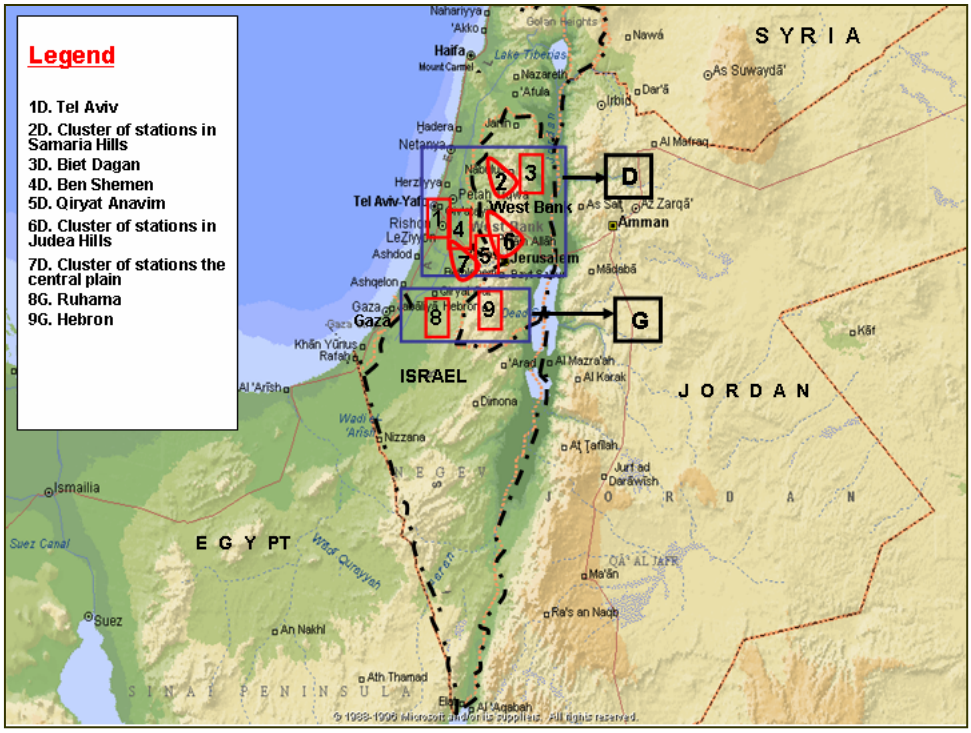

Figure 1: Map of the rain gauge locations in California and the land of Israel. The red frames represent the rain gauge locations and the irregular frames represent the cluster locations. The blue frames (A – G) represent different geographical areas. More details about those areas are given in figs. 10 and 11.

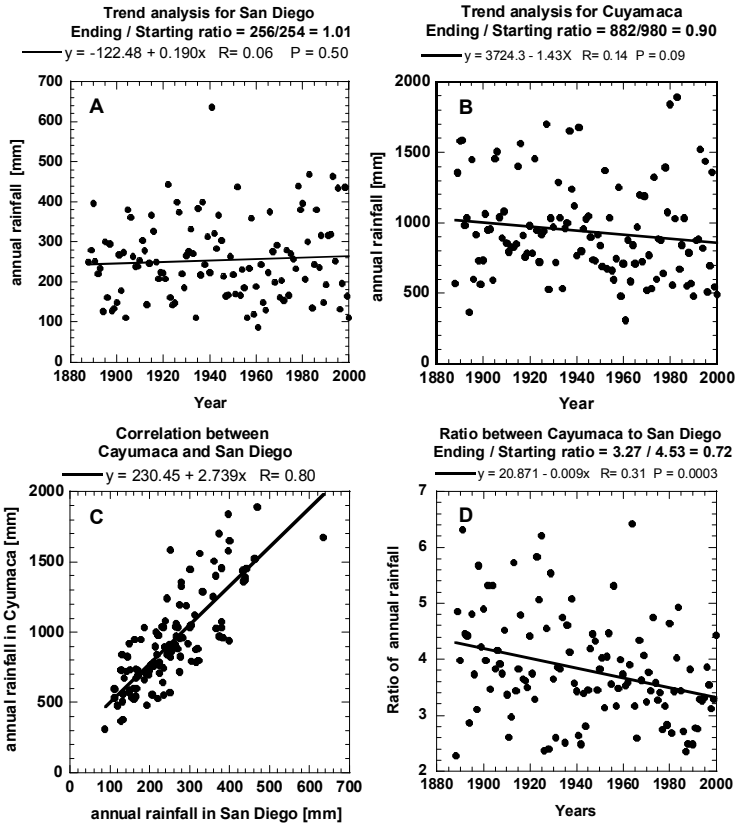

Figure 2: Long-range trends of the annual precipitation measured in San Diego (A) and in the downwind hilly station of Cuyamaca (B) at an elevation of 1550 m; the correlation between these two stations (C) and the annual ratio of precipitation (Ro) measured between them (D). The stations with the longest record in California are presented here. Note the sharp decrease in Ro with time in this area, which is affected by urban air pollution. Ending / Starting ratio means the ratio at the beginning of the time series compared to the ratio at the end, as calculated from the regression line at these times. R means the linear correlation coefficient and P is the statistical significance that corresponds to the t test statistic.

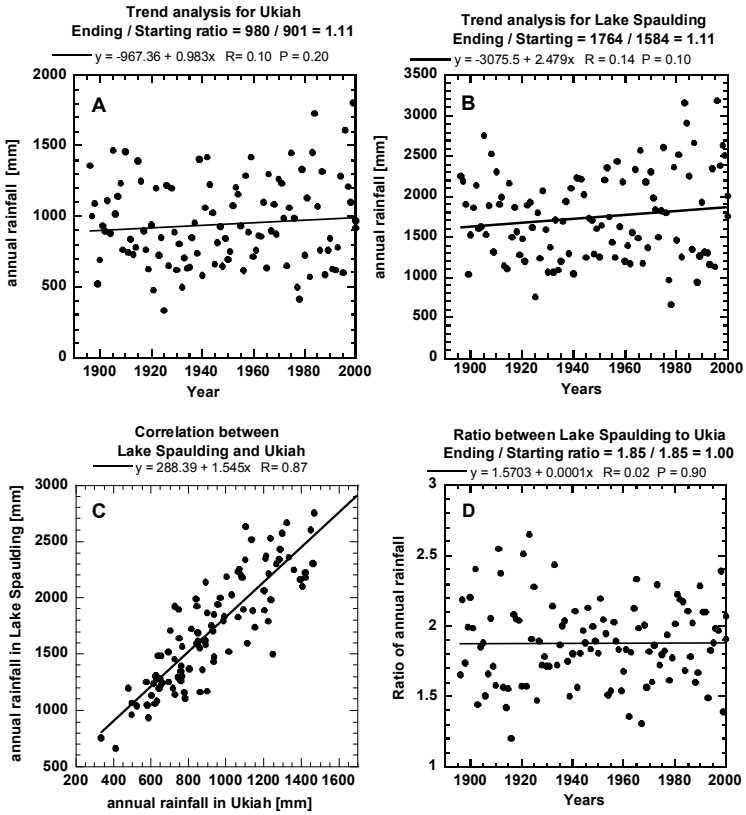

Figure 3: Same as Fig. 2, but for the relatively clean area in northern California at Ukiah (A) and the downwind hilly station of Lake Spaulding (B) at an elevation of 1717 m. The annual precipitation of the two stations is well correlated (C). Both stations show increases in precipitation over the period of record. Note the lack of a trend in the ratio between the hilly and upwind lowland stations (D).

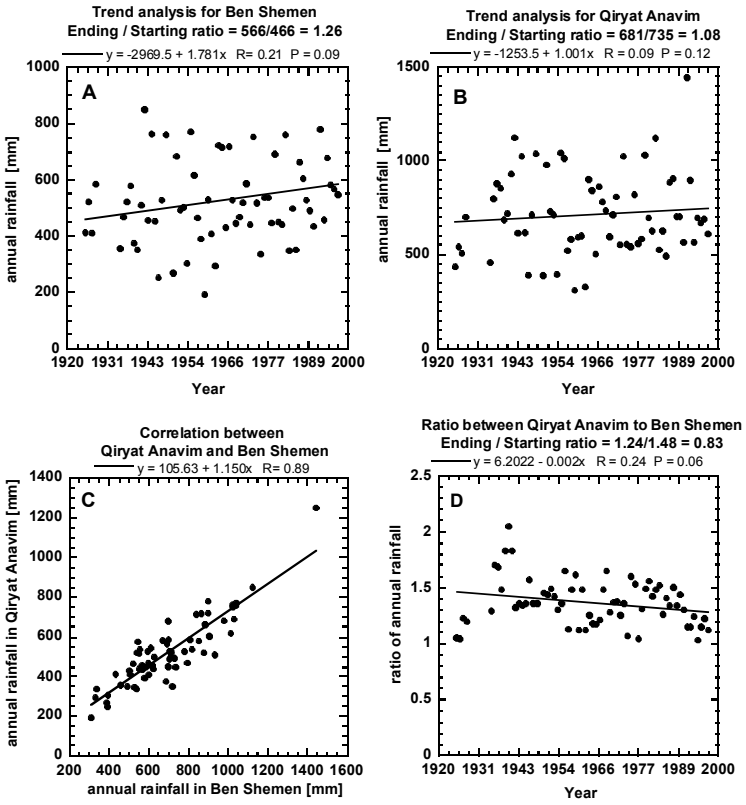

Figure 4: Same as Fig 2, but for a polluted region in the land of Israel, with the lowland station of Ben Shemen (A) and the downwind hilly station of Qiryat Anavim (B) at an elevation of 780 m. The annual rainfall of the two stations is well correlated (C). Both stations show increases in precipitation over the period of record Note the decreasing ratio between the two stations with time (D), as in the urban area in California (Fig. 2).

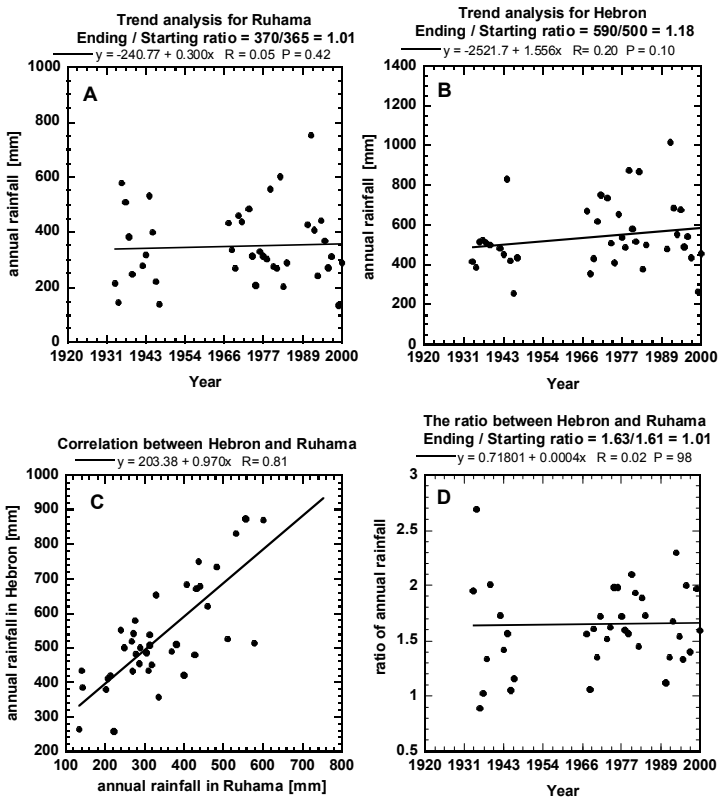

Figure 5: Same as Fig 2, but for a relatively unpolluted region in the land of Israel , with the lowland station of Ruhama (A) and the downwind hilly station of Hebron (B) at an elevation of 1000 m. Rainfall measurements in Hebron are not available for the years 1944-1966. Note the lack of trend in the ratio between the two stations with time (D), as in the clean area in northern California (Fig. 3).

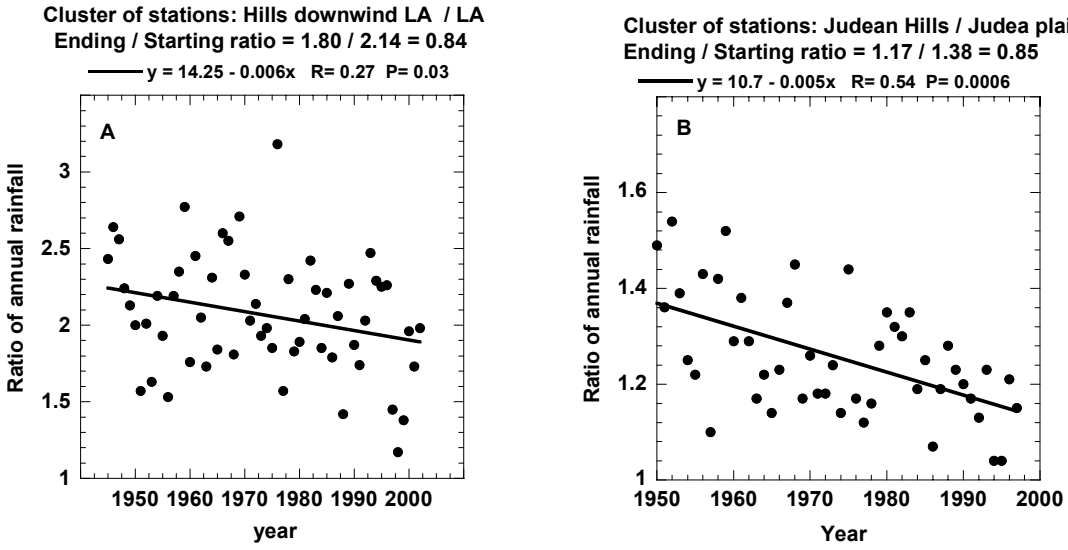

Figure 6 : Recent trends in the annual ratio of precipitation (Ro) between clusters of 5 to 7 gauges in the hills and the upwind urban area of (A) Los Angeles in California, and (B) the Judean hills vs. the Israel central coastal plain. The small P values show that the trends are statistically significant. Station details are in the appendix.

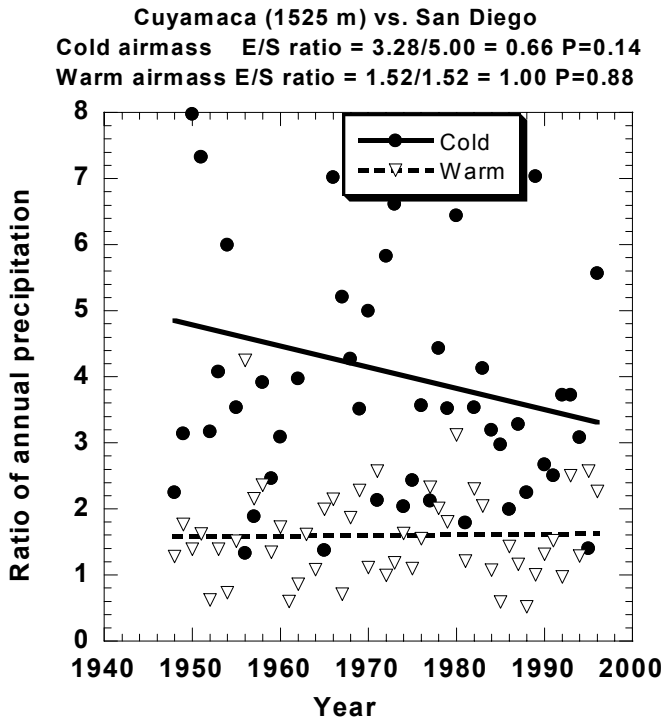

Figure 7: The annual ratios of precipitation (Ro) between Cuyamaca and San Diego for clouds occurring when T>-3°C at 700 hpa (mainly frontal and warm air mass) and when T ≤ -3°C (mainly cyclonic post frontal clouds).

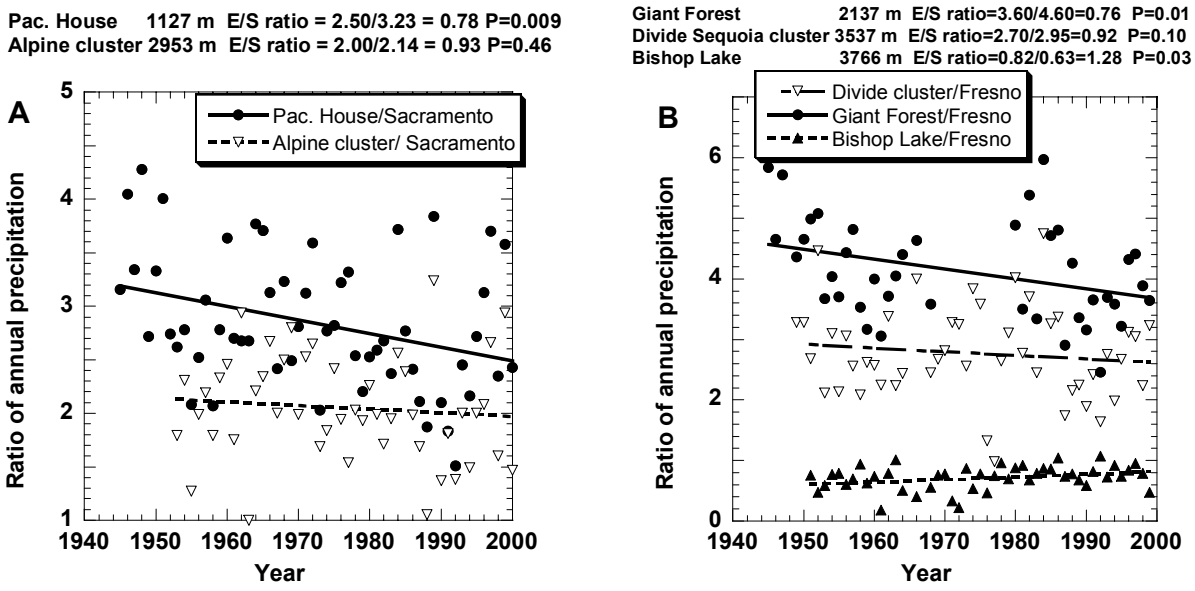

Figure 8: The annual ratios of precipitation (Ro) between the western slopes of the Sierra Nevada and the upwind lowlands, represented by (A) Pacific House versus Sacramento and (B) Giant Forest versus Fresno. The Ro of the water value of snow pack at highest western slopes of the Sierra Nevada is represented by Alpine cluster (Sonoma pass, Bond pass, Carson pass) versus Sacramento (A) and the cluster near the Divide above Sequoia-Kings National Park (Mono pass, Piute pass, Kaiser pass, Emerald Lake) versus Fresno (B). The relative compensation in the eastern slope is shown in B by Ro of Bishop Lake with respect to the Divide cluster.
The locations of the stations in A and B are shown in the blue frames A and B of Figure 1 and in maps A and B of Figure 10, respectively.

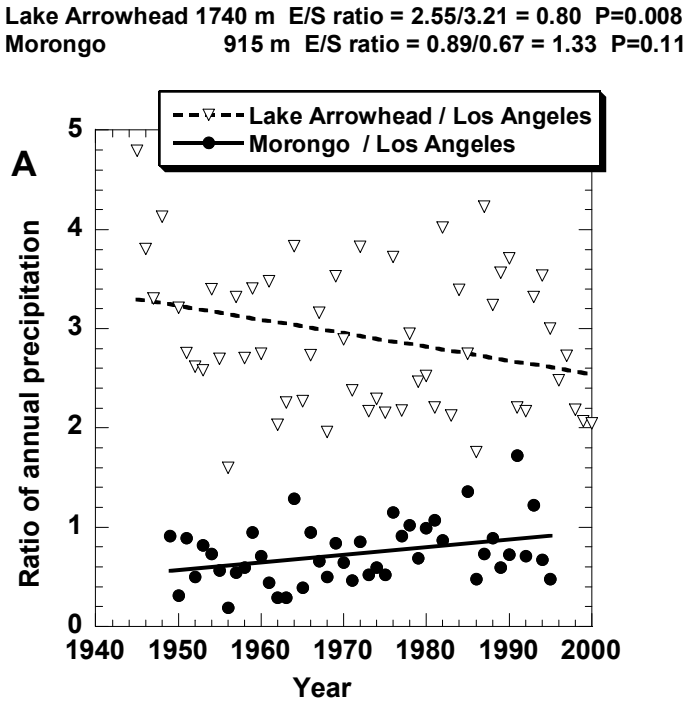

Figure 9: The annual ratios of precipitation (Ro) of rain gauges on the western slopes (Lake Arrowhead, 1740 m, 1033 mm/year, 22C in Fig.1) and eastern slopes (Morongo, 915 m, 244 mm/year, 23C in Fig 1) of the mountains to the east of Los Angeles with respect to the rainfall in Los Angeles. Note that the decreasing trend on the western slope is coupled with an increasing trend on the eastern slope.

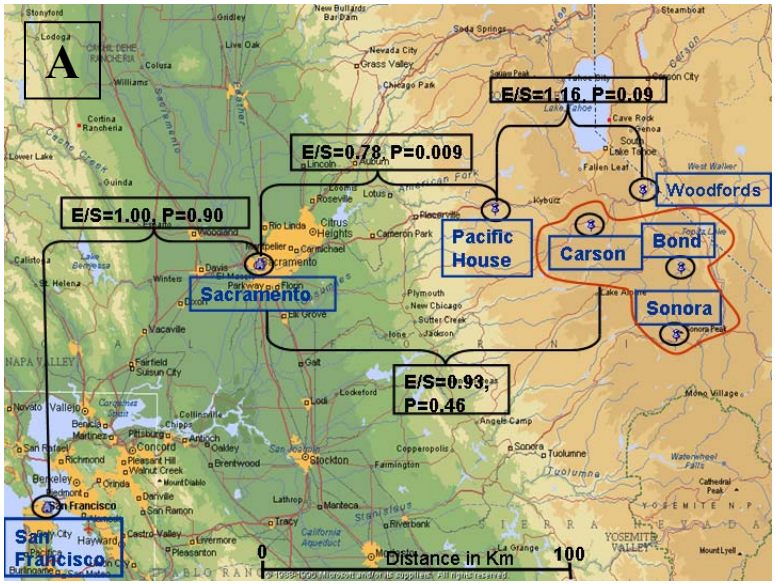
A
E/S=1.16, P=0.09
E/S=0.78, P=0.009
E/S=1.00, P=0.90
Woodfords
Pacific House
Carson
Bond
Sacramento
Sonora
E/S=0.93, P=0.46
San Francisco
0
Distance in Km
100

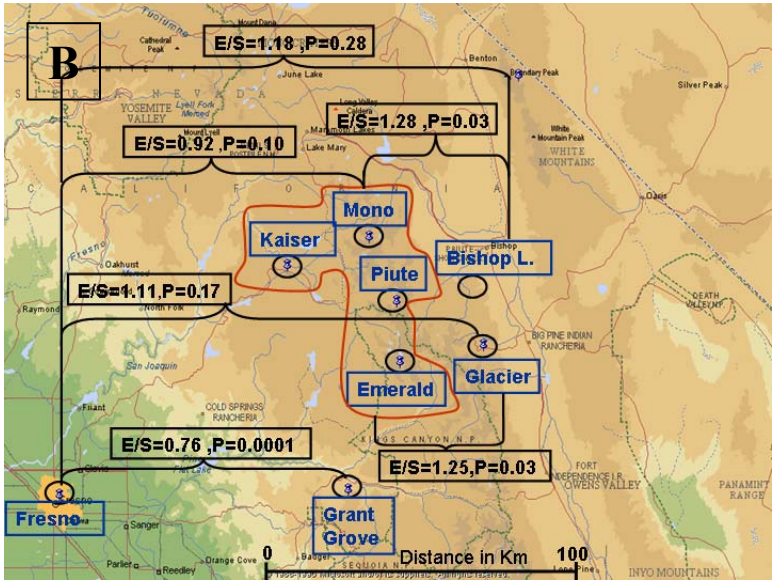
B
E/S=1.18 ,P=0.28
E/S=1.28 ,P=0.03
E/S=0.92 ,P=0.10
Mono
Kaiser
Bishop L.
Piute
E/S=1.11,P=0.17
Emerald
Glacier
E/S=0.76 ,P=0.0001
E/S=1.25,P=0.03
Fresno
Grant Grove
0
Distance in Km
100

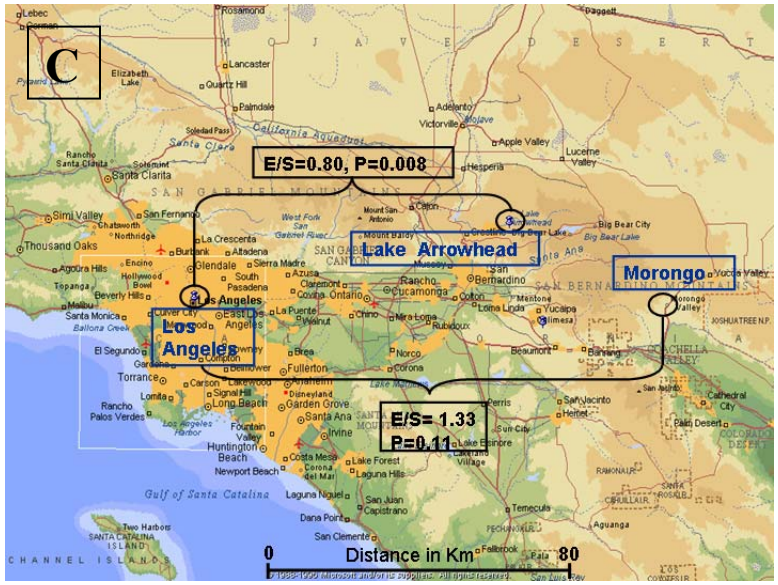
C
E/S=0.80, P=0.008
Lake Arrowhead
Morongo
Los Angeles
E/S= 1.33
P=0.11
0
Distance in Km
80

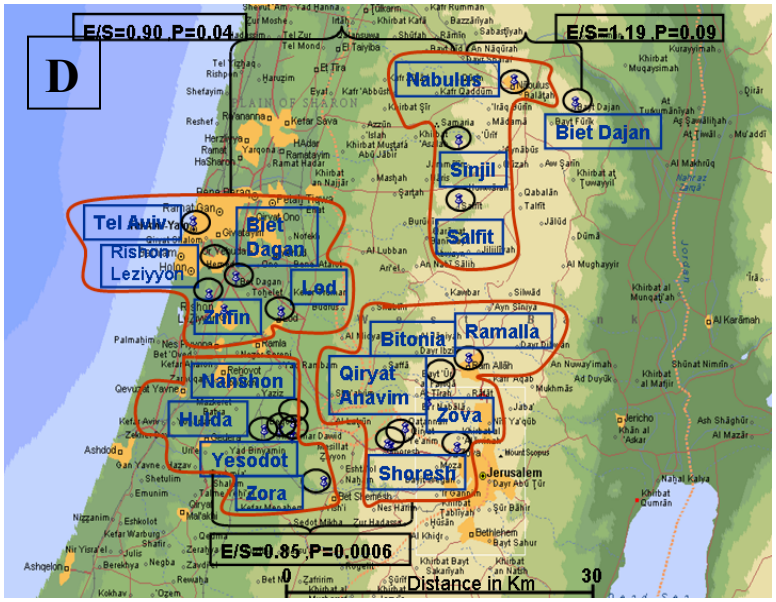
D
E/S=0.90 ,P=0.04
E/S=1.19 ,P=0.09
Nablus
Biet Dajan
Sinjil
Tel Aviv
Rishon Leziyyon
Biet Dagan
Salfit
Lod
Zrifin
Bitonia
Ramalla
Nahshon
Qiryat Anavim
Huda
Zova
Yesodot
Shoresh
Jerusalem
Zora
E/S=0.85 ,P=0.0006
0
Distance in Km
30

Figure 10: Summary of trends in precipitation ratios in cross sections downwind of urban areas. Map A shows the ratios of annual precipitation (Ro) for "polluted" rain gauges at a cross section downwind of Sacramento (6A in fig. 1) through the Pacific House (1147 m, 1308 mm/year) at the western slopes of the Sierra Nevada (7A in fig. 1), Cluster of snow pack stations (2953 m, 945 mm/year) at the divide in Alpine county (8A in fig. 1), Woodfords (1890 m, 533 mm/year) at the eastern slopes of the Sierra Nevada (9A in fig. 1). Map B shows a cross section downwind of Fresno (10B in fig. 1) through Grant Grove (2283 m, 1062 mm/year) at the western slopes of the Sierra (11B in fig. 1), cluster of snow pack stations (averaging 2953 m, 926 mm/year) in Sequoia-King N.P (12B in fig. 1), Glacier (2733 m, 406 mm/year) in the eastern slopes (13B in fig. 1), and Bishop Lake (3767, 546 mm/year) high in the eastern slopes (14B in fig. 1). Map C shows a cross section downwind of Los Angeles (19C in Fig. 1) through Lake Arrowhead (1740 m, 1033 mm/year) at the western slopes (21C in Fig. 1), Morongo (915 m, 244 mm/year) in the eastern slopes (23C in fig. 1). Map D shows a cross section downwind of Tel Aviv area (1D in Fig. 1) through a cluster of stations (660 m, 671 mm/year, 2D in Fig. 1) in the Samaria hills, and Biet Dajan (520 m, 320 mm/year, 3D in Fig. 1) in the eastern slopes. It also shows a cross section from a cluster of stations in the Israeli internal plain (180 m, 521 mm/year, 7D in Fig. 1) to a cluster of stations in the Judea hills (743 m, 650 mm/year, 6D in Fig. 1).

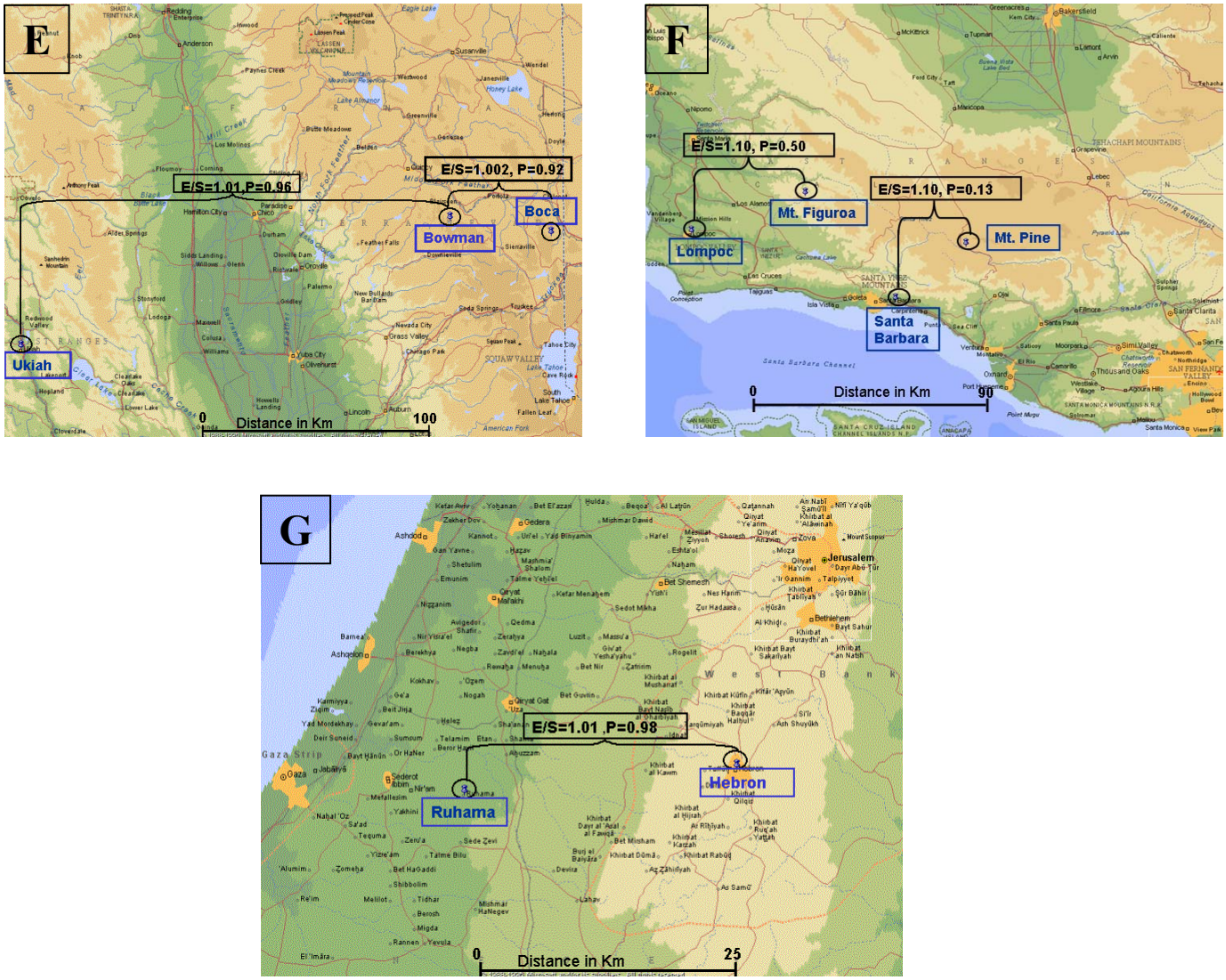

Fig 11: Same as fig. 10 but for a relatively pristine area. Map E shows the ratios of annual precipitation (Ro) in cross sections downwind of pristine areas in Northern California for Ukiah (208 m, 970 mm/year, 1E in fig. 1) through Bowman in the western slopes (2000 m, 1712 mm/year, 3E in fig.1), to Boca in the eastern slopes (1858 m, 572 mm/year, 4E in fig.1). Map F shows a cross section for two pairs of pristine stations to the north of Los Angeles: of Mt. Figuroa (1066 m, 508 mm/year, 16F in Fig. 1) versus Santa Barbara (33m, 524 mm/year, 15F in Fig. 1), and Mt. Pine (1400m, 575 mm/year, 18F in Fig. 1) versus Santa Barbara (33m, 524 mm/year, 17F in Fig. 1). Map G shows a cross section for Hebrom (1000 m, 560 mm/year, 9G in fig.1) in the Hebron hills versus Ruhama (150 m, 354 mm/year, 8G in fig.1), which is in Israel's southern plain and.

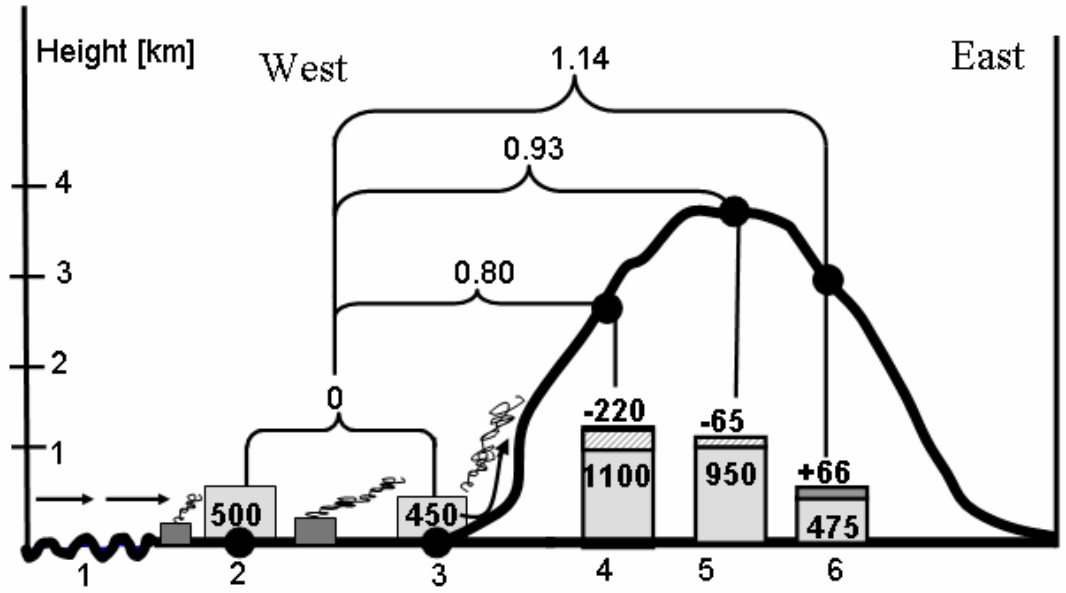

Fig 12: Topographic cross section showing the effects of urban air pollution on precipitation as the clouds move from west to east from the coast to the Sierra Nevada Mountains and to the eastern slopes. The boxes show the amount of the annual precipitation (mm/year) in each topographic location and the numbers above them show the loss or gain of precipitation (mm/year) at each site. Maritime air (zone 1) is polluted over coastal urban areas (zones 2, 3) - No decrease in precipitation occurs. The polluted air rises over mountains downwind and forms new polluted clouds (zone 4) – decreases of 15% -20% (losses of 220 mm/year) in the ratio between the western slopes to the coastal and plain areas. The clouds reach to the high mountains (zone 5). All the precipitation is snow – slight decrease of 5% to 7% (loss of 65 mm/year) in the ratio between the summits to the plain areas. The clouds move to the high eastern slopes of the range (zone 6) - increase of 14% (gain of 66 mm/year) in the ratio between the eastern slopes to the plain. According to Table 2 the net loss is dominant.

Tables

Table 1: Concentrations of non-sea salt ions in precipitation at the western slopes of the Sierra Nevada [micro equivalent liter^{-1}], and the respective precipitation loss [%] in adjacent rain gauges during the period 1945-2000. The ionic measurements are available from the National Atmospheric Deposition Program (NADP, 2003). The precipitation Ro changes are provided for Sequoia by the trend in the precipitation ratios of Giant Forest/ Fresno, for Yosemite by Pacific House/Sacramento, and for Lassen by Lake Spaulding / Ukiah. The full details of the precipitation trend analyses are available in the appendix.

Station	Elevation (m)	Period	All record	2001-2002	Trend μeq y^{-1}	Precip. Ro change %
Sequoia	1902	1981-2002	41.3	35.4	+0.311	-24
Yosemite	1408	1982-2002	30.7	36.5	-0.057	-22
Lassen Volcan	1765	2001-2002	---	17.7	---	0

Table 2: The approximate budget of precipitation change in the section with suppressed precipitation across the longitudinal zones of the Sierra Nevada, as defined in Fig. 12. The change in precipitated water volume is calculated for a 1-km wide strip across the mountains.

Zone	Description	Heights [m above sea level]	Width [km]	Rainfall change mm year-1	Rainfall change m^3
4	Western slopes	500-2500	100	-220	$-22x10^6$
5	Divide	> 2500	50	-65	$-3.25x10^6$
6	Eastern slopes	>2000	25	+66	$+1.65x10^6$
Total					$-23.60x10^6$